# Joint Neuroimage Synthesis and Representation Learning for Conversion Prediction of Subjective Cognitive Decline

Yunbi Liu[1,2], Yongsheng Pan[1], Wei Yang[2], Zhenyuan Ning[1,2], Ling Yue[3], Mingxia Liu[1(✉)], and Dinggang Shen[1(✉)]

[1] Department of Radiology and BRIC, University of North Carolina at Chapel Hill, Chapel Hill, NC 27599, USA
mxliu@med.unc.edu, Dinggang.Shen@gmail.com
[2] School of Biomedical Engineering, Southern Medical University, Guangzhou 510515, China
[3] Department of Geriatric Psychiatry, Shanghai Mental Health Center, Shanghai Jiao Tong University School of Medicine, Shanghai 200240, China

**Abstract.** Predicting the progression of preclinical Alzheimer's disease (AD) such as subjective cognitive decline (SCD) is fundamental for the effective intervention of pathological cognitive decline. Even though multimodal neuroimaging has been widely used in automated AD diagnosis, there are few studies dedicated to SCD progression prediction, due to challenges of *incomplete and limited data*. To this end, we propose a Joint neuroimage Synthesis and Representation Learning (JSRL) framework with transfer learning for SCD conversion prediction using incomplete multimodal neuroimaging data. Specifically, JSRL consists of two major components: 1) a generative adversarial network for synthesizing missing neuroimaging data, and 2) a classification network for learning neuroimage representations and predicting the progression of SCD. These two subnetworks share the same feature encoding module, encouraging that the to-be-generated representations are prediction-oriented and also the underlying association among multimodal images can be effectively modeled for accurate prediction. To handle the limited data problem, we further leverage both image synthesis and prediction models learned from a large-scale ADNI database (with MRI and PET acquired from 863 subjects) to a small-scale SCD database (with only MRI acquired from 113 subjects) in a transfer learning manner. Experimental results show that the proposed JSRL can synthesize reasonable PET scans and is superior to several state-of-the-art methods in SCD conversion prediction.

## 1 Introduction

As a self-reported experience of cognitive impairment, subjective cognitive decline (SCD) is one of the earliest noticeable symptoms of Alzheimer's disease (AD), mild cognitive impairment (MCI), and related dementia [1–5]. Considering that individuals with SCD are at increased risk of developing MCI or


A. L. Martel et al. (Eds.): MICCAI 2020, LNCS 12267, pp. 583–592, 2020.
https://doi.org/10.1007/978-3-030-59728-3_57

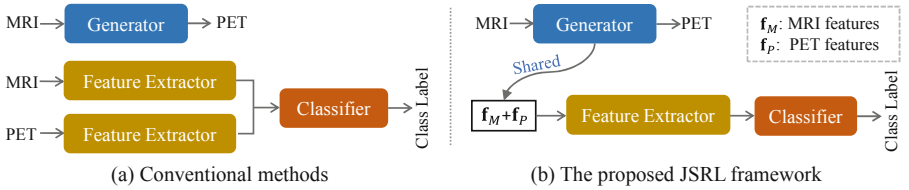


**Fig. 1.** Illustration of (a) conventional methods for separate neuroimage synthesis and representation learning and (b) the proposed Joint neuroimage Synthesis and Representation Learning (JSRL) framework for disease progression prediction using incomplete multimodal neuroimaging data (i.e., MRI and PET).

dementia [6], it is clinically meaningful to predict the progression of SCD for drug development and possible intervention of AD-related cognitive decline.

Existing studies have shown that structural magnetic resonance imaging (MRI) and positron emission tomography (PET) data contain complementary information to improve the performance of computer-aided brain disease diagnosis [7–9]. Unfortunately, compared with MRI, it is generally more difficult to obtain PET due to the relatively higher cost of PET scanning and other issues such as patients' concern about radioactive exposure. For instance, while all subjects in the public Alzheimer's Disease Neuroimaging Initiative (ADNI) have MRI data, only part of them have PET scans [10]. In the China Longitudinal Aging Social Survey (CLAS) dataset [11], all 113 subjects at 7 years' follow-up with definite conversion results have MRI scans but no PET data.

Previous studies usually discard subjects without PET scans, therefore significantly reducing the number of training samples and degrading the learning performance [12,13]. Recently, generative adversarial networks (GANs) have been employed to impute missing neuroimaging data [14,15], followed by multimodal representation learning and disease classification (see Fig. 1 (a)). Since image synthesis and representation learning are treated as two separate steps, these methods may lead to sub-optimal performance. Besides, existing methods often concatenate MRI and PET features for subsequent analysis, ignoring the underlying association between MRI and PET [16,17]. Intuitively, such association could be used as prior knowledge to boost the prediction performance. As shown in Fig. 1 (b), we propose to jointly perform image synthesis and representation learning for SCD conversion prediction, through which the underlying association between MRI and PET can be implicitly modeled.

In addition, we usually have very limited number of subjects for model learning. Directly training models on these limited data would degrade their robustness. To this end, we propose to leverage both image synthesis and prediction models learned from a large-scale ADNI database (with MRI and PET acquired from 863 subjects) to a small-scale SCD database (with only MRI from 113 subjects) in a transfer learning manner. The assumption is that, since SCD may be the preclinical stage of MCI and AD and AD/MCI is a progressive neurodegenerative disease, the discriminate brain changes between AD/MCI and normal controls (NCs) are potential biomarkers for SCD conversion prediction.

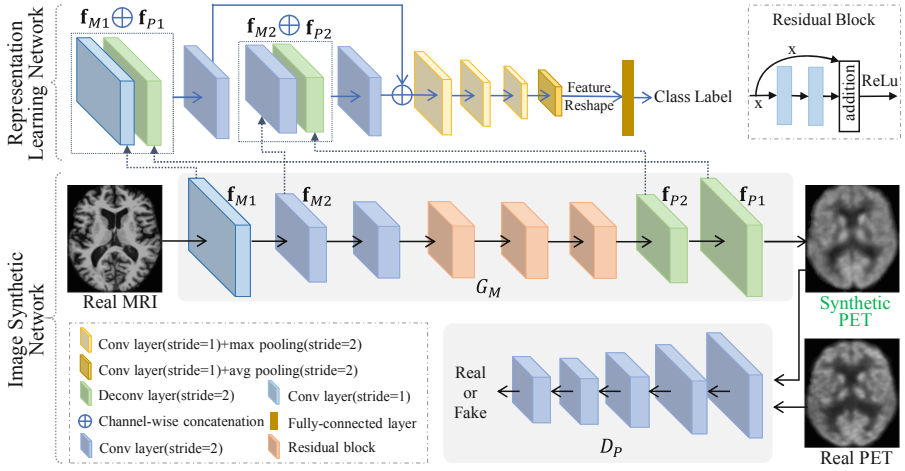


**Fig. 2.** Illustration of our JSRL framework for SCD conversion prediction, with a image synthesis network (bottom) and a representation learning network (top) for prediction. These two networks share the same feature maps, i.e., $[\mathbf{f}_{M1}, \mathbf{f}_{M2}]$ for MRI and $[\mathbf{f}_{P1}, \mathbf{f}_{P2}]$ for PET, encouraging that the to-be-generated representations are task-oriented for the prediction purpose. Conv: Convolution; Decov: Deconvolution.

The main contributions of this work can be summarized as follows: 1) A joint image synthesis and representation learning framework is proposed for predicting the progression of SCD subjects using incomplete multimodal neuroimaging data. This is different from previous approaches that discard data-missing subjects or treat image synthesis and feature learning as two separate tasks. 2) A transfer learning strategy is developed to handle the limited data problem, by leveraging knowledge learned from the ADNI to a small-scale SCD database.

## 2 Proposed Method

Our JSRL framework is illustrated in Fig. 2, containing 1) a generative adversarial network (GAN) for synthesizing missing neuroimages and generating multimodal features, and 2) a representation learning network for extracting imaging features and predicting the progression of brain disorders. These two subnetworks share the same features, i.e., $[\mathbf{f}_{M1}, \mathbf{f}_{M2}]$ for MRI and $[\mathbf{f}_{P1}, \mathbf{f}_{P2}]$ for PET, encouraging that the to-be-generated representations are prediction-oriented and the association between MRI and PET can be modeled.

**Problem Formulation.** In this work, we aim to utilize the domain knowledge learned from ADNI with MRI and PET scans to aid the conversion prediction of SCD with only MRI data. Let $\mathbf{I}_M$ denote the domain of MRI images and $\mathbf{I}_P$ be the domain of PET images. We denote a set of subjects (with paired MRI and PET scans) as $\mathcal{D} = \{(\mathbf{x}_M, \mathbf{x}_P) \,|\mathbf{x}_M \in \mathbf{I}_M, \mathbf{x}_P \in \mathbf{I}_P\}$. If no PET data is available,

one can resort to an image generator $G_M$: $\mathbf{I}_M \rightarrow \mathbf{I}_P$ to impute each PET based on its corresponding MRI. Based on the real MRI and synthesized PET data, a conventional multimodal prediction model is generally formulated as

$$y = C\left(\mathbf{x}_M, G_M\left(\mathbf{x}_M\right)\right), \tag{1}$$

where $y$ is the class label (e.g., stable SCD or progressive SCD) and $C$ is a classifier that tells whether an SCD subject will convert to MCI within a certain period. From Eq. 1, one can see that image synthesis and disease prediction are treated as two separate tasks. The JSRL can simultaneously perform image synthesis and prediction via a GAN model and a representation learning network, respectively. Based on the shared multimodal features (i.e., $\mathbf{f}_{M1}$, $\mathbf{f}_{M2}$ for MRI, and $\mathbf{f}_{P1}$, $\mathbf{f}_{P2}$ for PET), the prediction model can be formulated as

$$y = C\left(\mathbf{f}_{M1}, \mathbf{f}_{M2}, \mathbf{f}_{P1}, \mathbf{f}_{P2}\right). \tag{2}$$

**Joint Image Synthesis and Representation Learning.** Our JSRL has two subnetworks for joint image synthesis and prediction, with details given as below.

***1) Image Synthesis Network:*** We resort to a 3D GAN to synthesize missing neuroimages. Specifically, our image synthesis model contains a generator (i.e., $G_M$) and a discriminator (i.e., $D_P$). While the generator $G_M$ is used to impute missing PET images based on MRI scans, a discriminator is used to tell whether an input PET scan is real or not. As shown in the bottom of Fig. 2, the generator contains an encoder with 3 convolutional (Conv) layers, a transfer part with 3 residual blocks, a decoder with 2 deconvolutional (Deconv) layers, and an output layer. The channels of 3 Conv layers are 16, 32 and 64, respectively. For the sake of symmetry, the channels of two Deconv layers are the same as the corresponding Conv layers. The filter size of these Conv and Deconv layers is $3\times3\times3$ except the first Conv and the last Deconv layers with the filter size of $7 \times 7 \times 7$. Two types of loss functions are used in the image synthesis network, i.e., an adversarial loss and a reconstruction loss, defined as

$$\mathcal{L}(G_M) = \sum_{\{\mathbf{x}_M \in \mathbf{I}_M, \mathbf{x}_P \in \mathbf{I}_P\}} \left\|G_M(\mathbf{x}_M) - \mathbf{x}_P\right\|_1 + \log\left(1 - D_P(G_M(\mathbf{x}_M))\right), \tag{3}$$

where the 1st term is the reconstruction loss, and the 2nd term is the adversarial loss. For $D_P$, we need to minimize the loss

$$\mathcal{L}\left(D_P\right) = \sum_{\{\mathbf{x}_M \in \mathbf{I}_M, \mathbf{x}_P \in \mathbf{I}_P\}} \log(1 - D_P(\mathbf{x}_P)) + \log\left(D_P\left(G_M\left(\mathbf{x}_M\right)\right)\right). \tag{4}$$

***2) Representation Learning Network:*** To capture the association of different modalities, we develop a representation learning (RL) network to fuse multi-scale MRI and PET features for SCD conversion prediction. Since these two subnetworks share the same feature maps, one can encourage the to-be-generated

representations to be prediction-oriented. Specifically, to capture multi-scale feature representations of MRI and PET, we propose to share the feature maps of the first two Conv layers from the encoder (i.e., $\mathbf{f}_{M1}$ and $\mathbf{f}_{M2}$) in $G_M$ with RL for MRI, and share the feature maps of the last two Deconv layers from the decoder (i.e., $\mathbf{f}_{P1}$ and $\mathbf{f}_{P2}$) in $G_M$ with RL for PET. Then, the channel-wise concatenation of these multi-scale and multimodal feature maps are used as input of the RL network, as shown in the top of Fig. 2. Denote the concatenation of $\mathbf{f}_{M1}$ and $\mathbf{f}_{P1}$ as $C1$ and the concatenation of $\mathbf{f}_{M2}$ and $\mathbf{f}_{P2}$ as $C2$. As shown in the top of Fig. 2, $C1$ is followed by a Conv layer with a stride of 2 and $C2$ is followed by a Conv layer with a stride of 1. Then they are concatenated, followed by four Conv layers and a fully-connected (FC) layer. The first 3 and the last Conv layers are respectively followed by the max-pooling and average-pooling with the stride of 2 and they all have 16 channels with the filter size of $3 \times 3 \times 3$. Feature maps of the last Conv layer are reshaped into a feature vector, followed by an FC layer (with $1,280$ neurons) for classification/prediction. We use the cross-entropy loss in the RL network for classification, which is defined as

$$\mathcal{L}_R = -y \log p(\mathbf{x}) - (1-y) \log \left(1 - p(\mathbf{x})\right), \tag{5}$$

where $p(\mathbf{x})$ is the estimated probability of $\mathbf{x}$ belonging to the correct class $y$. For jointly training the generator and RL network, the overall loss JSRL is

$$\mathcal{L}_{total} = \mathcal{L}(G_M) + \lambda L_R, \tag{6}$$

where $\lambda$ is empirically set as 1.

**Transfer Learning Strategy.** To deal with the problem of limited training data, we develop a transfer learning solution, by leveraging knowledge from the relatively large-scale ADNI dataset to the small-scale CLAS dataset. Specifically, we design a *label transfer* strategy to augment the sample size for model training, as well as a *model transfer* strategy for missing neuroimage imputation and computer-aided SCD conversion prediction.

The CLAS contains stable SCD (sSCD) and progressive SCD (pSCD), while subjects in ADNI were divided into four categories: 1) AD, 2) NC, 3) MCI, and 4) SCD (i.e., subjective memory complaint). According to conversion results within 36 months, NC, MCI, SCD in ADNI can be further divided into sCN and pCN, sMCI and pMCI, sSCD and pSCD, respectively, with 'p' meaning progressive and 's' denoting stable. For example, 'pSCD' means that an SCD subject will convert to MCI within 36 months. Only 16 SCD subjects have definite conversion results (i.e., 11 pSCD and 5 sSCD) in ADNI. Since pCN and pSCD subjects would convert to MCI within a period, we assume that they have similar brain changes in their neuroimages. Accordingly, we propose to use sNC, pNC and MCI to aid SCD conversion prediction due to their close relationship (i.e., preclinical or prodromal stage of AD). Denote subjects belonging to the five categories (i.e., sNC, pNC, sSCD, pSCD, and MCI) as *SCD-adjacent subjects*. We reasonably regard sNC and sSCD as positive samples, and treat pNC, pSCD and MCI as

negative samples in ADNI. With such label allocation, we train JSRL for joint image synthesis and prediction on ADNI, and then apply the trained model to CLAS. Thus, the knowledge learned from ADNI can be transferred to CLAS for SCD conversion prediction.

**Implementation.** We first train the GAN (with $G_M$ and $D_P$) for 50 epochs, and then jointly train the generator $G_M$ and RL network for 30 epochs using 863 subjects with complete MRI and PET in ADNI. For GAN, we first train $G_M$ by minimizing $\mathcal{L}(G_M)$ with fixed $D_P$, and then train $D_P$ by minimizing $\mathcal{L}(D_P)$ with fixed $G_M$, iteratively. Then, we jointly train the generator $G_M$ and RL network by minimizing $\mathcal{L}_{total}$. The Adam solver with a learning rate of $2 \times 10^{-3}$ is used in the image synthesis network and a gradient descent optimizer with a learning rate of $10^{-2}$ is used in joint training of $G_M$ and RL network.

## 3 Experiments

**Datasets and Neuroimage Pre-processing.** The public Alzheimer's Disease Neuroimaging Initiative (ADNI)[1] database was studied in this work. We used MRI and PET data of 863 subjects (205 sNC, 29 pNC, 629 MCI) with complete MRI and PET scans from ADNI to train our JSRL network, and a validation set (containing 79 AD subjects with complete MRI and PET scans from ADNI) was used to validate the image synthesis model in our JRSL network. To validate the image synthesis model, we use AD subjects rather than SCD-adjacent subjects to make sure that all SCD-adjacent subjects with complete MRI and PET scans from the ADNI database can be used to train our representation learning network. We also collected a total of 113 SCD subjects (with only MRI data) in the CLAS database as an independent test set, including 73 sSCD and 40 pSCD subjects. All MRI and PET scans were pre-processed using a standard pipeline, including 1) skull-stripping via FreeSurfer, 2) intensity correction, and 3) spatial normalization to the Montreal Neurological Institute (MNI) space using SPM. After pre-processing, all images will have the same size as MNI.

**Experimental Setup.** In the *first* group of experiments, we evaluate the quality of synthetic images generated by the image synthesis network in JSRL. Specifically, we train the image synthesis model using 863 SCD-adjacent subjects with complete MRI and PET scans in ADNI, and test this image synthesis model on 113 SCD subjects with only MRI data in CLAS. Due to the lack of ground-truth PET images in CLAS, we further test this image synthesis model on 79 subjects with complete MRI and PET scans in ADNI to validate the reliability of our model. The averaged peak signal-to-noise (PSNR) and structure similarity image index (SSIM) are used to measure the quality of those synthetic images.

[1] http://adni.loni.usc.edu.

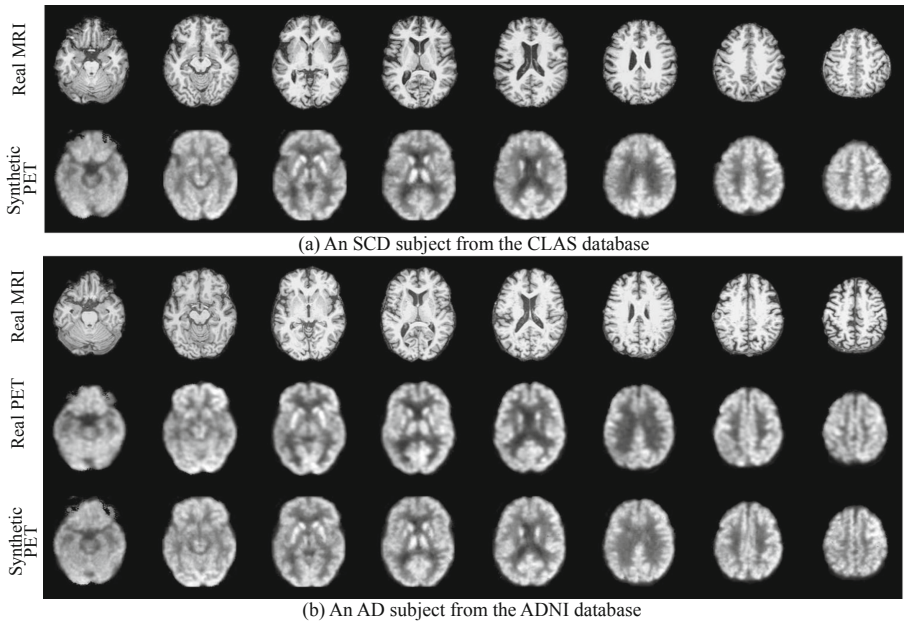


**Fig. 3.** Synthetic images generated by our method and their corresponding real images for two typical subjects from the CLAS and the ADNI databases.

In the *second* group, we evaluate the performance of our JSRL in SCD conversion prediction, by comparing JSRL with three conventional methods using handcrafted features, including 1) patch-based method (PBM) [18], 2) ROI-based pattern analysis (ROI) [19], and 3) landmark-based local energy patterns (LLEP) [20]. Note that features of MRI and PET data are concatenated in these four methods, followed by a linear support vector machine for prediction. We also compare JSRL with a state-of-the-art deep learning method, called disease-image specific neural network (DSNN) [14]. DSNN contains two subnetworks to extract MRI and PET features separately. Each subnetwork in DSNN consists of 5 Conv layers with a stride of 2 to extract MRI/PET features, and the MRI and PET features are further concatenated and reshaped into an FC layer for classification. Prediction models of all methods were trained on ADNI and tested on CLAS. The performance of SCD conversion prediction is measured by the area under the receiver operating characteristic (AUC), accuracy (ACC), sensitivity (SEN), specificity (SPE), and F1-Score(F1S).

**Results of Neuroimage Synthesis.** We first evaluate the quality of synthetic images generated by our GAN subnetwork in JSRL. Here, the GAN model is first trained on 863 SCD-adjacent subjects with complete PET and MRI from ADNI, and then tested on 113 subjects (with MRI only) from CLAS. Due to the lack of ground-truth PET images in CLAS, we show the visual results of the synthetic

**Table 1.** Results achieved by four methods in SCD conversion prediction (i.e., sSCD vs. pSCD classification), with models trained on ADNI and tested on CLAS. Methods marked as "-M" denote that only subjects with MRI in ADNI are used for training, while the remaining methods employ all subjects in ADNI with complete MRI and PET for training, and the real MRI and synthetic PET in CLAS for test.

| Method | AUC | ACC | SPE | SEN | F1S |
|---|---|---|---|---|---|
| ROI-M | 0.597 | 0.611 | **0.699** | 0.450 | 0.450 |
| PBM-M | 0.500 | 0.443 | 0.397 | 0.525 | 0.400 |
| LLEP-M | 0.510 | 0.487 | 0.493 | 0.475 | 0.396 |
| DSNN-M | 0.590 | 0.522 | 0.452 | 0.650 | 0.490 |
| ROI | 0.603 | 0.584 | 0.658 | 0.450 | 0.434 |
| PBM | 0.538 | 0.496 | 0.425 | 0.625 | 0.467 |
| LLEP | 0.516 | 0.451 | 0.500 | 0.425 | 0.392 |
| DSNN | 0.557 | 0.558 | 0.589 | 0.500 | 0.444 |
| JSRL (ours) | **0.713** | **0.655** | 0.616 | **0.725** | **0.598** |

PET images. A subject from CLAS with real MRI and synthetic PET is shown in Fig. 3 (a). One can observe that our synthetic PET images look reasonable in appearance. We also test this model on 79 validation subjects (with paired MRI and PET) from ADNI. A subject from ADNI with real MRI, real PET, and synthetic PET is shown in Fig. 3 (b), suggesting that our synthetic PET image looks similar to its real one. The mean SSIM and PSNR values of synthetic PET on ADNI are 0.85 and 23.22, respectively. This suggests that our image synthesis model is reasonable and the synthetic PET scans have acceptable image quality.

**Results of SCD Conversion Prediction.** We further compare our JSRL with five competing methods in SCD conversion prediction, with results reported in Table 1. From Table 1, we can have following observations. 1) The proposed transfer learning strategy works well in SCD conversion prediction (with AUCs $> 0.5$ for most methods). 2) Methods with multimodal data generally outperform their single-modal counterparts in terms of AUC values. This suggests that our synthesized PET scans are helpful in boosting the prediction performance. 3) JSRL outperforms conventional handcrafted feature based methods (i.e., ROI, PBM, and LLEP) and the deep learning method (i.e., DSNN), validating the effectiveness of the proposed framework for joint image synthesis and representation learning. 4) JSRL achieves a significantly improved SEN value (i.e., 0.725), which is 7.5% higher than the second-best SEN (i.e., 0.650) achieved by DSNN-M. In real-world applications, the high sensitivity of JSRL may be very useful for accurately identifying subjects with progressive SCD.

## 4 Conclusion and Future Work

In this paper, we present a joint neuroimage synthesis and representation learning (JSRL) framework for SCD conversion prediction based on incomplete multimodal neuroimages. Specifically, JSRL consists of a GAN model for imputing missing neuroimages and a representation learning network for SCD conversion prediction. We also develop a transfer learning strategy to handle the limited data problem, by leveraging knowledge learned from the relatively large-scale ADNI database to the small-scale CLAS database. Experimental results suggest that JSRL can synthesize PET scans with reasonable image quality and also achieve good results in SCD conversion prediction. Our study indicates that the JSRL framework and transfer learning strategy can be potentially applied to the early detection of preclinical AD, which needs to be verified in future work. Currently, we directly apply JSRL trained on ADNI to CLAS using a label transfer and model transfer strategy. Designing advanced data adaptation methods [21] is expected to explicitly alleviate the data distribution difference between these two databases, which will be our future work.

**Acknowledgements.** This work was finished when Y. Pan was visiting the University of North Carolina at Chapel Hill. Y. Liu and Y. Pan contributed equally to this work.

## References

1. Jessen, F., et al.: A conceptual framework for research on subjective cognitive decline in preclinical Alzheimer's disease. Alzheimer's Dement. **10**(6), 844–852 (2014)
2. Amariglio, R.E., et al.: Subjective cognitive complaints and amyloid burden in cognitively normal older individuals. Neuropsychologia **50**(12), 2880–2886 (2012)
3. Buckley, R.F., et al.: A conceptualization of the utility of subjective cognitive decline in clinical trials of preclinical Alzheimer's disease. J. Mol. Neurosci. **60**(3), 354–361 (2016). https://doi.org/10.1007/s12031-016-0810-z
4. Kryscio, R.J., et al.: Self-reported memory complaints: implications from a longitudinal cohort with autopsies. Neurology **83**(15), 1359–1365 (2014)
5. Liu, M., Zhang, J., Yap, P.T., Shen, D.: View-aligned hypergraph learning for Alzheimer's disease diagnosis with incomplete multi-modality data. Med. Image Anal. **36**, 123–134 (2017)
6. Mitchell, A., Beaumont, H., Ferguson, D., Yadegarfar, M., Stubbs, B.: Risk of dementia and mild cognitive impairment in older people with subjective memory complaints: meta-analysis. Acta Psychiatrica Scandinavica **130**(6), 439–451 (2014)
7. Kawachi, T., et al.: Comparison of the diagnostic performance of FDG-PET and VBM-MRI in very mild Alzheimer's disease. Eur. J. Nuclear Med. Mol. Imaging **33**(7), 801–809 (2006). https://doi.org/10.1007/s00259-005-0050-x
8. Zu, C., Jie, B., Liu, M., Chen, S., Shen, D., Zhang, D.: Label-aligned multi-task feature learning for multimodal classification of Alzheimer's disease and mild cognitive impairment. Brain Imaging Behav. **10**(4), 1148–1159 (2016). https://doi.org/10.1007/s11682-015-9480-7
9. Liu, M., Zhang, J., Adeli, E., Shen, D.: Landmark-based deep multi-instance learning for brain disease diagnosis. Med. Image Anal. **43**, 157–168 (2018)

10. Jack Jr, C.R., et al.: The Alzheimer's disease neuroimaging initiative (ADNI): MRI methods. J. Mag. Reson. Imaging: Off. J. Int. Soc. Magn. Reson. Med. **27**(4), 685–691 (2008)
11. Yue, L., et al.: Asymmetry of hippocampus and amygdala defect in subjective cognitive decline among the community dwelling Chinese. Front. Psychiatry **9**, 226 (2018)
12. Frisoni, G.B., Fox, N.C., Jack, C.R., Scheltens, P., Thompson, P.M.: The clinical use of structural MRI in Alzheimer disease. Nat. Rev. Neurol. **6**(2), 67–77 (2010)
13. Jie, B., Liu, M., Liu, J., Zhang, D., Shen, D.: Temporally constrained group sparse learning for longitudinal data analysis in Alzheimer's disease. IEEE Trans. Biomed. Eng. **64**(1), 238–249 (2016)
14. Pan, Y., Liu, M., Lian, C., Xia, Y., Shen, D.: Spatially-constrained Fisher representation for brain disease identification with incomplete multi-modal neuroimages. IEEE Trans. Med. Imaging **39**, 2965–2975 (2020)
15. Yi, X., Walia, E., Babyn, P.: Generative adversarial network in medical imaging: a review. Med. Image Anal. **58**, 101552 (2019)
16. Cheng, B., Liu, M., Zhang, D., Munsell, B.C., Shen, D.: Domain transfer learning for MCI conversion prediction. IEEE Trans. Biomed. Eng. **62**(7), 1805–1817 (2015)
17. Cheng, B., Liu, M., Shen, D., Li, Z., Zhang, D.: Multi-domain transfer learning for early diagnosis of Alzheimer's disease. Neuroinformatics **15**(2), 115–132 (2017). https://doi.org/10.1007/s12021-016-9318-5
18. Coupé, P., Eskildsen, S.F., Manjón, J.V., Fonov, V.S., Collins, D.L.: Simultaneous segmentation and grading of anatomical structures for patient's classification: application to Alzheimer's disease. NeuroImage **59**(4), 3736–3747 (2012)
19. Rusinek, H., et al.: Alzheimer disease: measuring loss of cerebral gray matter with MR imaging. Radiology **178**(1), 109–114 (1991)
20. Zhang, J., Liu, M., Shen, D.: Detecting anatomical landmarks from limited medical imaging data using two-stage task-oriented deep neural networks. IEEE Trans. Image Process. **26**(10), 4753–4764 (2017)
21. Wang, M., Zhang, D., Huang, J., Yap, P.T., Shen, D., Liu, M.: Identifying autism spectrum disorder with multi-site fMRI via low-rank domain adaptation. IEEE Trans. Med. Imaging **39**(3), 644–655 (2019)